J. Chem. Soc., Faraday Trans. 1, 1981, **77**, 2465-2479

Kinetics of Chlorine Oxide Radical Reactions using Modulated Photolysis

Part 4.—The Reactions $Cl + Cl_2O \rightarrow Cl_2 + ClO$ and $ClO + HO_2 \rightarrow$ Products Studied at 1 atm and 300 K

BY JOHN P. BURROWS* AND RICHARD A. COX

Environmental and Medical Sciences Division, A.E.R.E., Harwell, Oxfordshire OX11 0RA

Received 25th September, 1980

Rate coefficients for the reactions,

$$HO_2 + ClO \rightarrow HOCl + O_2 \quad (1a)$$

$$\rightarrow HCl + O_3 \quad (1b)$$

$$Cl + Cl_2O \rightarrow Cl_2 + ClO \quad (2)$$

have been determined by studying the modulated photolysis of mixtures of Cl_2, Cl_2O, H_2, O_2 and N_2 at 300 K and 1 atm total pressure. HO_2 and ClO were observed by u.v. absorption spectroscopy and kinetic information was obtained by monitoring the in-phase and in-quadrature absorption components as a function of photolysis period. The values obtained for k_1 and k_2 were:

$$k_1 = (5.4^{+4}_{-2}) \times 10^{-12}\ cm^3\ molecule^{-1}\ s^{-1}$$

$$k_2 = (1.0 \pm 0.35) \times 10^{-10}\ cm^3\ molecule^{-1}\ s^{-1}.$$

An upper limit for the pathway (1*b*) was determined by observing the production of ozone in the reaction mixture:

$$k_{1b} \leqslant 1.5 \times 10^{-14}\ cm^3\ molecule^{-1}\ s^{-1}.$$

The potential depletion of atmospheric ozone by man-made pollutants necessitates a detailed understanding of the chemistry of the stratosphere.[1-3] ClO and HO_2 are important free-radical constituents of the stratosphere, where they participate in chemical reactions, which, in part, determine the concentration of ozone. Reactions which convert reactive species such as Cl and ClO into less reactive compounds such as HOCl and HCl are particularly interesting, as they may have a relatively large effect on the calculated amount of ozone depletion in the stratosphere, resulting from the release of chlorofluorocarbons at the earth's surface. The reaction between ClO and HO_2 is potentially of this kind, since the stable products of the exothermic channels of this reaction, paths 1(*a*) and 1(*b*), both offer a possible sink for active chlorine species:

$$ClO + HO_2 \rightarrow HOCl + O_2 \quad \Delta H_{1a} = -180\ kJ\ mol^{-1} \quad (1a)$$

$$ClO + HO_2 \rightarrow HCl + O_3 \quad \Delta H_{1b} = -50\ kJ\ mol^{-1} \quad (1b)$$

$$ClO + HO_2 \rightarrow \text{products}. \quad (1c)$$

Investigations of the disproportionation reactions of HO_2[4-6] and ClO[7,8] have demonstrated the complex nature of apparently simple bimolecular reactions undergone by these radicals. During the course of this study three investigations of reaction (1) have been reported, all using the low-pressure discharge-flow technique, and

detecting species either by resonance fluorescence,[9] laser magnetic resonance (l.m.r.),[10] or mass spectrometry.[11] The l.m.r. study has shown that reaction (1) exhibits a complicated temperature dependence, which is inconsistent with a simple H atom transfer mechanism and suggests complex behaviour similar to that exhibited by HO_2 and ClO in their self-disproportionation reactions. The possibility therefore arises that k_1 may be pressure dependent. One of the principal aims of this study was to determine the value of k_1 at 1 atm pressure. It was also intended to determine the extent of any O_3 production from the exothermic pathway, reaction (1*b*). Recently O_3 formation has been observed as a minor channel in the self-disproportionation of CH_3COO_2,[12] presumably *via* a complex intermediate which might be analogous to that required by reaction (1*b*).

Here some investigations of reaction (1) using the molecular modulation technique are reported. The method adopted for studying reaction (1) necessitated the production of HO_2 and ClO at approximately equal rates by the modulated photolysis of mixtures of Cl_2, Cl_2O, H_2, O_2 and N_2. The formation and subsequent decay processes of HO_2 and ClO in the system were investigated by observing the phase lag of the radicals behind the modulated photolysis light source. In order to determine the ClO production rate in the system, it was initially necessary to measure the rate coefficient for the reaction

$$Cl + Cl_2O \rightarrow Cl_2 + ClO. \qquad (2)$$

This reaction is believed to have little importance in the chemistry of the stratosphere. The formation of O_3 by reaction (1*b*) was investigated by flowing the reaction mixture after photolysis into a chemiluminescence analyser. The detection of O_3 enabled an upper limit to be determined for k_{1b}.

EXPERIMENTAL

A detailed description of the molecular modulation technique and the spectrometer used is given elsewhere.[13] However, a schematic diagram of the apparatus is shown in fig. 1. The square-wave modulated light source was provided by up to 5 fluorescent blacklamps ($310 < \lambda/\text{nm} < 400$), Philips TL 40/08, mounted radially around the jacketed quartz reaction vessel, which had an effective path length of 120 cm with 2.5 cm diameter windows at each end. U.v. absorptions were monitored using a collimated beam from a deuterium lamp which passed along the axis of the cell and through a spectrometer onto a photomultiplier (EMI 9783). Modulated absorptions were measured as separate in-phase and in-quadrature components using a digital lock-in detector.

The HO_2 radical was observed at 220 nm using a small double monochrometer (Spex Doublemate) with a spectral width of 1.1 nm. The HO_2 absorption cross-section used, σ_{HO_2} (220 nm) $= 3.5 \times 10^{-18}$ cm^2, was determined in a study of the HO_2 disproportionation reaction.[5] At this wavelength the absorption cross-section of Cl_2O is relatively small [σ_{Cl_2O} (220 nm) $= 9 \times 10^{-20}$ cm^2][14] and consequently interference from absorption by this reactant is insignificant. However, at 277.2 nm (the wavelength of the band-head of the 11-0 band of the $A \leftarrow X$ system of ClO, which is used to monitor ClO) appreciable absorption by Cl_2O occurs. It was therefore necessary to use a differential absorption technique to observe ClO. By suitable positioning of two photomultipliers in the focal plane of the spectrometer, both the absorption at the band-head of the 11-0 band of ClO and the background absorption just off the band were simultaneously observed. These signals were combined in an amplifier (Keithley 604) and the resultant differential signal was fed to the digital lock-in device. The signals for ClO were calibrated by producing ClO in the photolysis of Cl_2 and O_2 mixtures, and observing ClO absorption both directly and differentially at 277.2 nm.[7] In this manner an effective differential absorption cross-section for ClO of 3.2×10^{-18} cm^2 was obtained based on an absolute absorption cross-section of 7.26×10^{-18} cm^2[14] at this wavelength. The differential

signals had inherently more noise than the direct observation. Combined with the lower absorption cross-section this resulted in a factor of *ca.* 4 difference in sensitivity between the two methods of observation. The ClO data were therefore of a lower precision than the HO_2 data; this is reflected in the sum of the squares of residuals for computed fits to experimental data for ClO behaviour and HO_2 behaviour (see below).

Experimental mixtures contained Cl_2, Cl_2O, H_2, O_2 and N_2, typical concentrations being 1×10^{16}, 2×10^{15}, 1.8×10^{19}, 4×10^{18} and 1.3×10^{18} molecule cm^{-3}, respectively. Individual gas-flows were measured for H_2, O_2 and N_2 using calibrated rotameters. The Cl_2 and Cl_2O

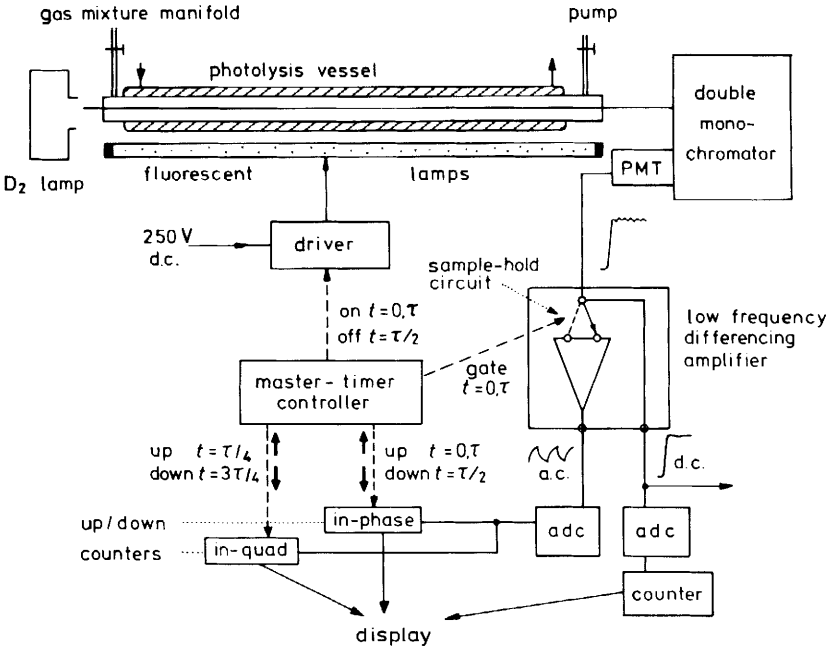

FIG. 1.—Schematic diagram of the molecular modulation apparatus.

concentrations were determined within the reaction vessel by u.v. absorption. The pressure in the reaction vessel was measured using a pressure transducer (MKS Baratron 170M-6B). H_2 (cylinder grade), N_2 (high-purity grade), O_2 (breathing grade) and 5% Cl_2 in N_2 (high-purity grade) were supplied by British Oxygen Co. The O_2 was further purified by passage over copper oxide at 670 K to remove hydrocarbon impurities, and then dried by passing the gas through a molecular sieve. The Cl_2O was prepared continuously by passing Cl_2 in N_2 over yellow HgO.[15]

The rate of photochemical decomposition of Cl_2 was determined by measuring the rate of decay of Cl_2 when mixtures of Cl_2, H_2 and O_2 were photolysed.[16] The photolysis rates for Cl_2O and OClO were calculated by comparing the Cl_2 absorption with the Cl_2O or OClO absorption over the observed output intensity and wavelength distribution of the photolysis lamp.

O_3 production in the photolysis of Cl_2, Cl_2O, H_2, O_2 and N_2 mixtures was monitored by flowing the reaction mixture from the reaction vessel into a chemiluminescence analyser, where the gas flow (*ca.* 1 dm^3 min^{-1}) was mixed with a small flow of ethylene (13 cm^3 min^{-1}). The resultant emission was used to monitor the O_3 concentration in the exit gas. The instrument was calibrated by measuring optically at 254 nm concentrations of O_3 in the reaction vessel and then flowing this gas into the chemiluminescent analyser. The emission was shown to be linearly proportional to $[O_3]$ in the range 10^{13}-10^{14} molecule cm^{-3} and the minimum detectable value of $[O_3]$ was *ca.* 1×10^{10} molecule cm^{-3}.

TABLE 1.—CHEMICAL REACTIONS USED IN COMPUTER SIMULATION

chemical reactions	k (300 K) /cm^3 molecule^{-1} s^{-1}	ref.
(a) basic chemical scheme:		
(1) $ClO + HO_2 \rightarrow$ products	5.4×10^{-12}	this work[a]
(2) $Cl + Cl_2O \rightarrow Cl_2 + ClO$	1.0×10^{-10}	this work[a]
(3) $HO_2 + HO_2 \rightarrow H_2O_2 + O_2$	2.35×10^{-12}	(5)
(4) $ClO + ClO \rightarrow Cl_2 + O_2$	8.2×10^{-15}	this work[a]
(5) $Cl_2 + h\nu \rightarrow Cl + Cl$	1.4×10^{-3}[c]	this work[a]
(10) $Cl + H_2 \rightarrow HCl + O_2$	1.5×10^{-14}	(19)-(22)
(11) $H + O_2 + M \rightarrow HO_2 + M$	5.9×10^{-32}[d]	(31)
(b) additional chemistry:		
(6) $Cl_2O + h\nu \rightarrow ClO + Cl$	2.88×10^{-4}	this work[b]
(7) $ClO + ClO \rightarrow Cl + ClOO$	7.2×10^{-15}	(18)
(8) $ClO + ClO \rightarrow Cl + OClO$	8.0×10^{-15}	(18)
(9) $ClO + ClO + M \rightleftharpoons Cl_2O_2 + M$	1.16×10^{-14}[e]	(7)
(12) $OClO + h\nu \rightarrow O + ClO$	3.2×10^{-2}	this work[b]
(13) $O + O_2 + M \rightarrow O_3 + M$	5.6×10^{-34}[d]	(31)
(14) $Cl + O_2 + M \rightleftharpoons ClOO + M$	5.04×10^{-21}[e]	(13)
(15) $O + Cl_2O \rightarrow ClO + ClO$	4.1×10^{-12}	(30)
(16) $O + ClO \rightarrow Cl + O_2$	5.0×10^{-11}	(14)
(17a) $Cl + ClOO \rightarrow Cl_2 + O_2$	9.8×10^{-11}	(13)
(17b) $Cl + ClOO \rightarrow ClO + ClO$	4.5×10^{-12}	(13)
(18) $Cl + OClO \rightarrow ClO + ClO$	5.9×10^{-11}	(14)
(19) $Cl + Cl_2O_2 \rightarrow Cl_2 + ClOO$	1.0×10^{-11}	(13)
(23) $Cl + HO_2 \rightarrow HCl + O_2$	4.9×10^{-11}	(31)

[a] Measured; [b] calculated; [c] s^{-1}; [d] cm^6 molecule^{-1} s^{-1}; [e] cm^3 molecule^{-1}.

The in-phase and in-quadrature absorption components, obtained from the digital lock-in counters, are related to the time varying concentration of the absorber $R(t)$ by the expressions

$$P = C\sigma l\left[\int_0^{\tau/2} R(t)\,\mathrm{d}\tau - \int_{\tau/2}^{\tau} R(t)\,\mathrm{d}\tau\right] \tag{A}$$

$$Q = C\sigma l\left[\int_{\tau/2}^{3\tau/2} R(t)\,\mathrm{d}\tau - \int_{3\tau/2}^{5\tau/2} R(t)\,\mathrm{d}\tau\right] \tag{B}$$

where P and Q represent the in-phase and in-quadrature counting rates, C is a calibration factor, σ is the absorption cross section, l the path length and τ the photolysis period. For radicals undergoing simple first- or second-order kinetic behaviour, the function $R(t)$ can be obtained by exact integration of the appropriate differential equations describing the behaviour of the radical in the system. Subsequent exact solution of eqn (A) and (B) enables P and Q to be expressed as functions of the quantities $2B$, the rate of production of radicals, k, the appropriate decay rate coefficient for the radical, σ, l and τ.

In more complex chemical systems with mixed kinetic order, where two different radicals react together, exact integration of the differential equations describing their chemical behaviour is no longer possible and integration must be done by numerical methods. This approach was used to derive the separate absorption components, P and Q, for HO_2 and ClO. The concentrations of these radicals are determined by the equations:

for lights on,

$$\frac{\mathrm{d}[HO_2]}{\mathrm{d}t} = B - k_1[ClO][HO_2] - 2k_3[HO_2]^2$$

$$\frac{\mathrm{d}[ClO]}{\mathrm{d}t} = B - k_1[ClO][HO_2] - 2k_4[ClO]^2$$

for lights off,

$$\frac{d[HO_2]}{dt} = -k_1[ClO][HO_2] - 2k_3[HO_2]^2$$

$$\frac{d[ClO]}{dt} = -k_1[ClO][HO_2] - 2k_4[ClO]^2$$

where $B = k_5[Cl_2]$ under experimental conditions and k_1, k_3 and k_4 are radical reaction rate coefficients.

The Harwell computer program FACSIMILE[17] was used to compute the HO_2 and ClO concentrations and obtain their in-phase and in-quadrature absorption components. The chemical scheme used for integration is listed in table 1.

For qualitative discussion of the radical behaviour, it is constructive to consider the relative magnitude of P and Q as a function of photolysis period τ. If τ is long compared with the radical lifetime T, then the radical behaviour will tend towards a square-wave form in-phase with the photolysis lamps and $P \gg Q$. If τ is comparable with T then $P \approx Q$, and if τ is smaller than T, then $P \ll Q$. A useful concept, obtained from molecular modulation investigations of free-radical chemistry, is the lifetime parameter τ_0, the period at which the in-phase and in-quadrature components are equal. This occurs when the radical has a phase lag of $\pi/4$ radians. For first- or second-order kinetic behaviour of a radical, τ_0 is simply related to the rate coefficient for radical decay.[13]

RESULTS

Mixtures of Cl_2 and Cl_2O, when photolysed using blacklamps ($310 < \lambda/\text{nm} < 400$) generate radicals *via* the reactions

$$Cl_2 + h\nu \rightarrow Cl + Cl \tag{5}$$

$$Cl + Cl_2O \rightarrow ClO + Cl_2 \tag{2}$$

and also to a minor extent ($\lesssim 4\%$) by the photolysis of Cl_2O

$$Cl_2O + h\nu \rightarrow Cl + ClO. \tag{6}$$

The ClO in such systems reacts *via* the following processes:

$$ClO + ClO \rightarrow Cl_2 + O_2 \tag{4}$$

$$ClO + ClO \rightarrow Cl + ClOO \tag{7}$$

$$ClO + ClO \rightarrow Cl + OClO \tag{8}$$

$$ClO + ClO + M \rightleftharpoons Cl_2O_2 + M. \tag{9}$$

These reactions have been studied in detail,[7,8,18] and in the $Cl_2 + Cl_2O$ system, ClO behaviour at 300 K in the molecular modulation apparatus is best described by an effective overall second-order loss, which is here assigned to reaction (4). This is because the products of reactions (7)-(9) regenerate ClO.

Consider the photolysis of mixtures of Cl_2 and Cl_2O in the presence of H_2 and O_2. HO_2 and ClO radicals are produced by the reactions

$$Cl_2 + h\nu \rightarrow Cl + Cl \tag{5}$$

$$Cl + H_2 \rightarrow HCl + H \tag{10}$$

$$H + O_2 + M \rightarrow HO_2 + M \tag{11}$$

$$Cl + Cl_2O \rightarrow ClO + Cl_2. \tag{2}$$

Providing the ratio $[H_2]/[Cl_2O] \leqslant 10^3$, then reaction (2) dominated the consumption of Cl atoms and reaction (4) dominated the decay of ClO. Under these conditions, ClO in-phase and in-quadrature absorption components were measured as a function of photolysis period τ, and the effective overall second-order rate coefficient for loss of ClO was determined at 300 K,

$$k_4 = (8.2 \pm 2.0) \times 10^{-15}\ \mathrm{cm^3\ molecule^{-1}\ s^{-1}}.$$

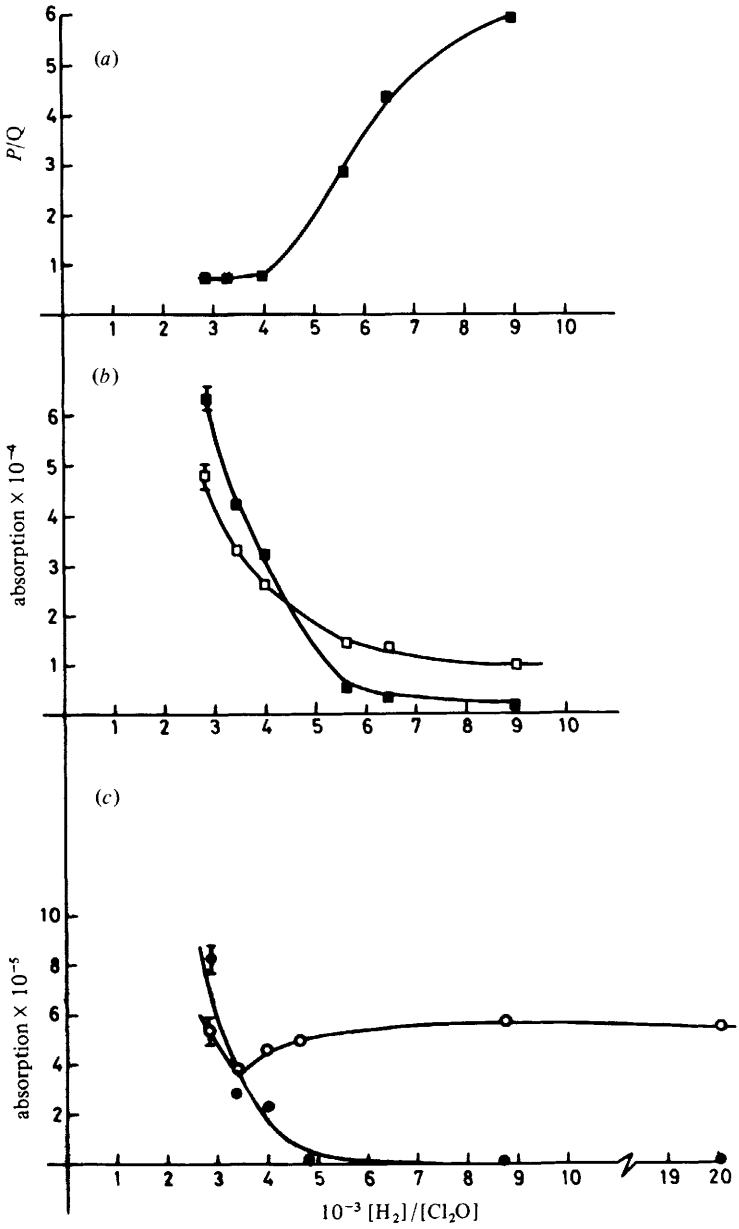

FIG. 2.—In-phase (P) and in-quadrature (Q) absorptions as a function of $[H_2]/[Cl_2O]$ at $\tau = 4$ s: (a) P/Q (■) for the ClO absorption at 277.2 nm are plotted as ordinate; (b) P (□) and Q (■) absorptions at 277.2 nm are plotted as ordinate; (c) P (○) and Q (●) absorptions at 220 nm are the ordinate.

As the ratio $[H_2]/[Cl_2O]$ was increased, reaction (10) started competing with reaction (2) for consumption of Cl atoms, HO_2 being formed subsequently *via* reaction (11). Using a fixed photolysis period ($\tau = 4.0$ s), the in-quadrature absorption component for ClO was observed to decrease both in absolute magnitude and relative to the in-phase absorption component, as the $[H_2]/[Cl_2O]$ ratio was increased [see fig. 2(*b*)]. This reflected the increasing production of HO_2 and resultant decrease in the lifetime of ClO in the system, as the fast reaction (1) began dominating over the slow disproportionation reaction (4).

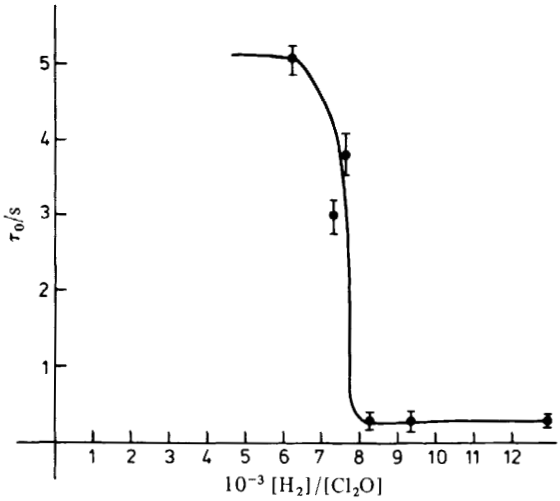

FIG. 3.—Plot of τ_0 for ClO against $[H_2]/[Cl_2O]$ ratio.

At high $[Cl_2O]$, the absorption at 220 nm, where HO_2 was monitored, was complicated by the presence of another absorbing species, which exhibited strong in-quadrature signals, typical of a slow reacting transient [see fig. 2(*c*)]. This absorption is tentatively assigned to Cl_2O_2 as its behaviour qualitatively followed that of ClO, which does not absorb appreciably at this wavelength [σ_{ClO} (220 nm) $\approx 6 \times 10^{-19}$ cm^2].[14] However, as the $[H_2]/[Cl_2O]$ ratio increased, the Cl_2O_2 signals disappeared, leaving an in-phase signal ascribed to HO_2. When $k_{11}[H_2]$ was greater than $k_2[Cl_2O]$, the HO_2 decay was determined by reactions (1) and (3)

$$HO_2 + HO_2 \rightarrow H_2O_2 + O_2. \qquad (3)$$

Measurement of k_2: $Cl + Cl_2O \xrightarrow{k_2} Cl_2 + ClO$

Experimentally it was observed that the appearance of HO_2 signals and the change from $P/Q < 1$ to $P/Q > 1$ for ClO behaviour, at long photolysis period ($\tau = 4$ s), occurred abruptly as the $[H_2]/[Cl_2O]$ ratio was increased. As a first approximation, it was assumed that the rate of reactions (1) and (10) were equal at the midpoint of the P/Q against $[H_2]/[Cl_2O]$ plot depicted in fig. 2(*a*). This enabled an estimate of the ratio of k_1/k_{10} to be made:

$$\frac{k_2}{k_{10}} = \left(\frac{[H_2]}{[Cl_2O]}\right)_{\text{midpoint } P/Q} \approx 6 \times 10^3.$$

The plot of the lifetime parameter τ_0 for ClO also showed a marked dependence on $[H_2]/[Cl_2O]$ ratio (see fig. 3). Assuming that the rates of reactions (2) and (10) are

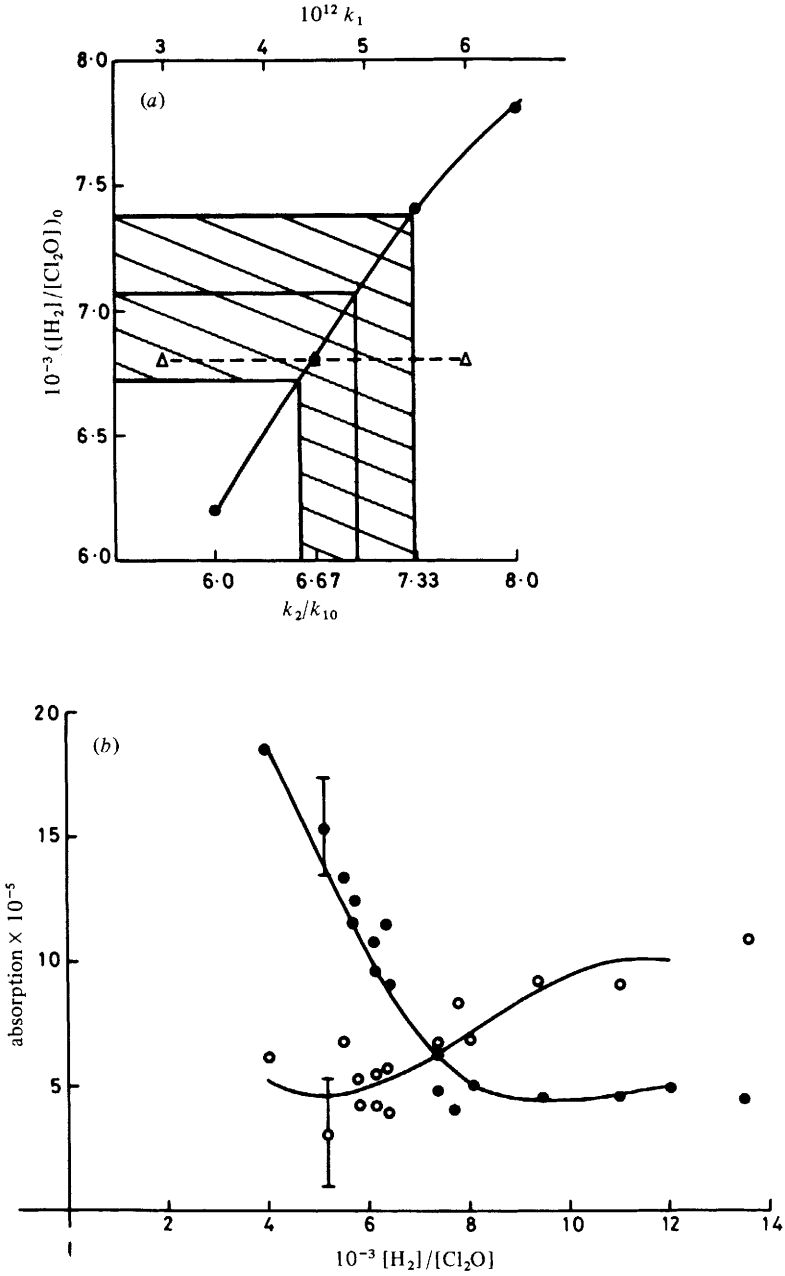

FIG. 4.—(*a*) Plot of the computed $([H_2]/[Cl_2O])_0$ ratio against either the value for k_2/k_{10} (—●—) or the value used for the rate coefficient k_1 (--△--) in the simulation. (*b*) In-phase (*P*, ○) and in-quadrature (*Q*, ●) absorption components plotted against $[H_2]/[Cl_2O]$ ratio. The line is a computed simulation using the chemistry listed in table 1 and setting $k_1 = 5.4 \times 10^{-12}$ cm^3 molecule^{-1} s^{-1} and $k_2 = 1.0 \times 10^{-10}$ cm^3 molecule^{-1} s^{-1}.

equal at the mid-point of the τ_0 changes with $[H_2]/[Cl_2O]$, a second estimate for k_2/k_{10} can be made:

$$\frac{k_2}{k_{10}} = \left(\frac{[H_2]}{[Cl_2O]}\right)_{\text{midpoint } \tau_0} \approx 7.6 \times 10^3.$$

The data shown in fig. 4(*b*) are in-phase and in-quadrature absorption components for ClO as a function of $[H_2]/[Cl_2O]$, obtained using a photolysis period of $\tau = 1$ s. The lines plotted on this diagram represent computer simulations of the absorption components using the chemical scheme listed in table 1. The data shown in fig. 4(*b*) are qualitatively similar to that shown in fig. 2(*b*) obtained with $\tau = 4$ s. Experimentally it was found that at $\tau = 1$ s, the crossover of the in-phase and in-quadrature signals for ClO occurred at $([H_2O]/[Cl_2O])_0 = (7.07 \pm 0.35) \times 10^3$. The in-phase and in-quadrature absorption components for ClO were computed as a function of $[H_2]/[Cl_2O]$, at a fixed photolysis period of 1 s, using different values of k_1 and k_2. The calculated $([H_2]/[Cl_2O])_0$ at the crossover point was independent of k_1 in the range (3-6) $\times 10^{-12}$ cm^3 molecule^{-1} s^{-1} but was almost linearly dependent on the ratio k_2/k_{10} as is shown in fig. 4(*a*). Comparison with the experimentally determined values for $([H_2]/[Cl_2O])_0$ gave

$$k_2/k_{10} = (6.9 \pm 0.5) \times 10^3.$$

Using the mean of four recent determinations of k_{10} at 298 K[19-22] *i.e.*:

$$k_{10} = (1.5 \pm 0.5) \times 10^{-14} \text{ cm}^3 \text{ molecule}^{-1} \text{ s}^{-1}$$

yields the following value for k_2

$$k_2 = (1.0 \pm 0.35) \times 10^{-10} \text{ cm}^3 \text{ molecule}^{-1} \text{ s}^{-1} \text{ at 300 K}.$$

Measurement of k_1: $HO_2 + ClO \xrightarrow{k_1}$ products

Having determined the value of k_2/k_{10}, the $[H_2]/[Cl_2O]$ ratio was chosen so that the HO_2 production was slightly in excess of the ClO production. This resulted in the ClO decay being dominated by reaction (1) with only a small flux of radicals through reaction (4). Under these conditions the HO_2 behaviour was determined by both reaction (1) and reaction (3).

In-phase and in-quadrature absorption components for both HO_2 and ClO were measured as a function of τ, in the photolysis of mixtures of Cl_2 and Cl_2O with H_2, O_2 and N_2 present. Typical results are shown in fig. 5 and 6, where the curves plotted correspond to the computer simulated absorption components using $k_1 = 6.0 \times 10^{-12}$ cm^3 molecule^{-1} s^{-1}. Similar curves were generated using a variety of values for k_1. A best fit value for k_1 was obtained by finding the minimum in the sum of the squares of the residuals $[\Sigma(x - x^1)^2]$ between the experimental data and computed absorptions. This fit is shown in fig. 7, where x represents the computed value for P and Q and x^1 is the measured P and Q. Minima were obtained for both HO_2 and ClO data at the same value of k_1. Unfortunately the sum of the squares of the residuals for the ClO is always higher than that for the HO_2, due to its inherently noisier signal. This probably accounts for the second minimum in the sum of squares of residuals for the ClO data. From the HO_2 and ClO data a value for k_1 was determined at 300 K:

$$k_1 = (5.4^{+4}_{-2}) \times 10^{-12} \text{ cm}^3 \text{ molecule}^{-1} \text{ s}^{-1}.$$

Measurement of k_{1b}: $HO_2 + ClO \xrightarrow{k_{1b}} HCl + O_3$

Ozone was observed in the photolysis of Cl_2, Cl_2O, H_2, O_2 and N_2 mixtures by flowing the reaction mixture after photolysis into a chemiluminescent analyser. The

O_3 was monitored as a function of the $[H_2]/[Cl_2O]$ ratio, at a fixed photolysis period $\tau = 1$ s. The results obtained are shown in fig. 8. $[O_3]$ depends on the ratio $[H_2]/[Cl_2O]$ in a manner similar to the case of ClO absorption [see fig. 2(*b*)]. At low $[H_2]/[Cl_2O]$ values, $[O_3]$ was apparently proportional to the $[ClO]^2$, which is consistent with its formation *via* the reactions

$$ClO + ClO \rightarrow Cl + OClO \tag{8}$$

$$OClO + h\nu \rightarrow O + ClO \tag{12}$$

$$O + O_2 + M \rightarrow O_3 + M. \tag{13}$$

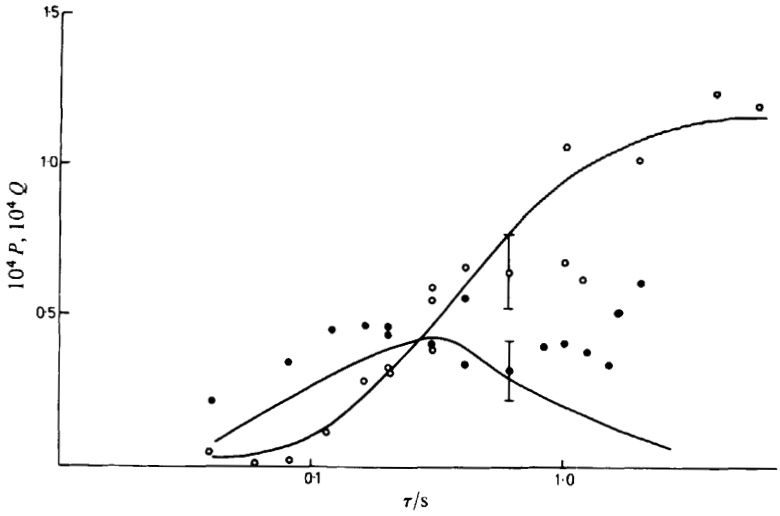

FIG. 5.—In-phase (P, ○) and in-quadrature (Q, ●) absorption components for HO_2 at 220 nm plotted against τ/s. The line drawn represents a computer simulation of P and Q, using the chemistry in table 1 with $k_1 = 6 \times 10^{-12}$ cm^3 molecule^{-1} s^{-1} and $k_2 = 1.0 \times 10^{-10}$ cm^3 molecule^{-1} s^{-1}.

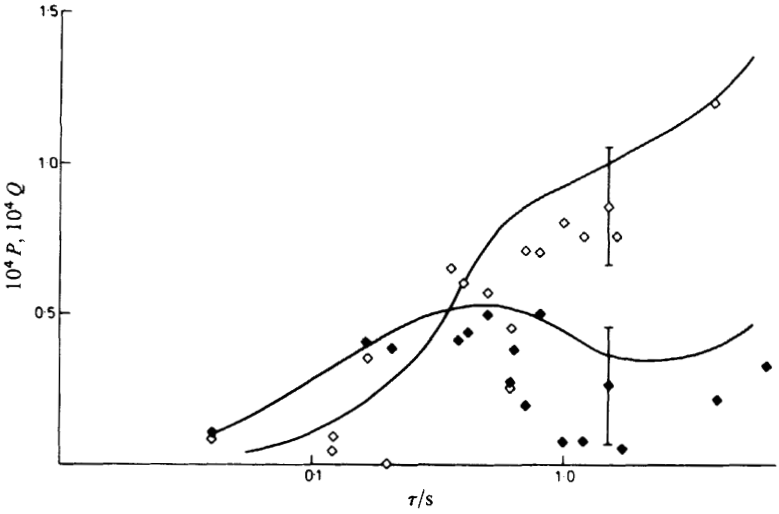

FIG. 6.—In-phase (P, ◇) and in-quadrature (Q, ◆) absorption components plotted against τ/s. The line drawn represents a computed simulation of P and Q using the chemistry in table 1 with $k_1 = 6 \times 10^{-12}$ cm^3 molecule^{-1} s^{-1} and $k_2 = 1.0 \times 10^{-10}$ cm^3 molecule^{-1} s^{-1}.

Owing to the presence of a relatively large production of O_3 resulting from the ClO disproportionation, determination of the extent of the O_3 production from reaction (1 *b*) was difficult. The value of $[O_3]$ measured is that of the O_3 at the exit point from the reaction vessel. Since on entry to the vessel there is no ozone, and assuming that the rate of production of O_3 within the vessel is linear, then the observed O_3 can be related to the rate of formation of O_3, F, by the equation

$$F = \frac{[O_3]_{obs}}{\Delta t}$$

where $[O_3]_{obs}$ is the measured concentration of O_3 in the exit gas at the chemiluminescence analyser and Δt is the residence time for the reaction mixture in the vessel.

An upper limit for reaction (1 *b*) was calculated in the following manner. A value of $[H_2]/[Cl_2O]$ (*ca.* 6×10^3) was chosen near to the point where the rates of production of HO_2 and ClO were equal. The rate F, calculated at this value of $[H_2]/[Cl_2O]$, was

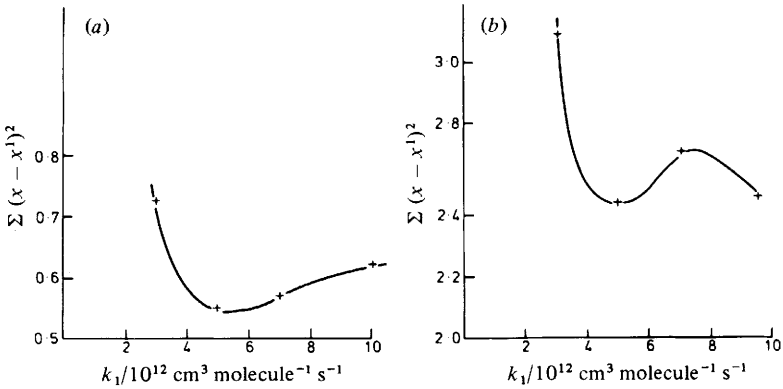

FIG. 7.—Sum of the squares of residuals $\Sigma(x-x^1)^2$, between the computed absorption components x and the experimental data x^1 for HO_2 (*a*) and ClO (*b*) plotted against the value used for k_1 in the simulation.

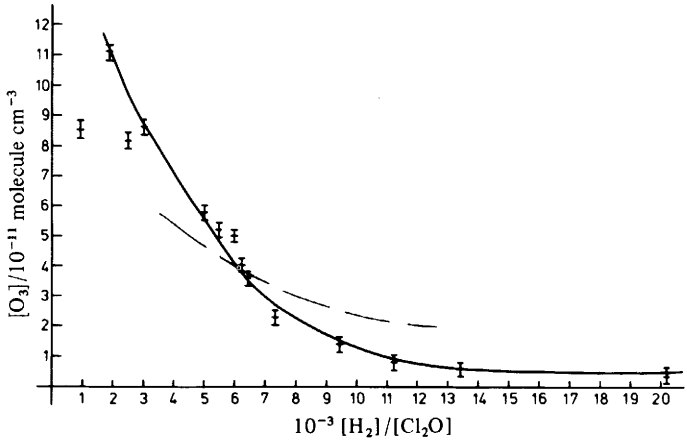

FIG. 8.—Plot of $[O_3]$ observed against $[H_2]/[Cl_2O]$. The bold line is drawn through the experimental data. The dashed line (---) is the computed value of $[O_3]$ using the chemistry listed in table 1 using values of $k_1 = 5.4 \times 10^{-12}$ cm³ molecule⁻¹ s⁻¹, $k_2 = 1.0 \times 10^{-10}$ cm³ molecule⁻¹ s⁻¹ and $k_{1b} = 1.5 \times 10^{-14}$ cm³ molecule⁻¹ s⁻¹.

compared with the total mean computed flux through reaction (1) over the time Δt. This yielded

$$k_{1b} \leqslant 1.5 \times 10^{-14}\ \text{cm}^3\ \text{molecule}^{-1}\ \text{s}^{-1}.$$

This value of k_{1b} was then employed in a computer simulation in which the amount of O_3 formed from all sources after Δt s reaction time was calculated. The complete reaction scheme given in table 1 was used in this simulation. The computed amount of O_3 is compared with that obtained experimentally in fig. 8 and it can be seen that the model overestimates the observed O_3 at high values of $[H_2]/[Cl_2O]$. This suggests that the true value of k_{1b} is substantially lower than the upper limit value given above.

DISCUSSION

The chemical reactions used to simulate the modulated photolysis of the Cl_2, Cl_2O, H_2, O_2 and N_2 mixtures are shown in table 1. The most important reactions, which govern the HO_2 and ClO concentrations, are those listed in section (*a*) of table 1. The addition of the chemical reactions listed in section (*b*) to the chemical scheme changed the predicted in-phase and in-quadrature absorptions for HO_2 and ClO by $< 5\%$. The reaction of H with HO_2, producing either 2OH or H_2 and O_2, was insignificant in the system, as the concentration of H atoms never exceeded 1×10^7 molecule cm^{-3}. This is due to the very rapid reaction removal of H atoms by reaction with O_2. Consider the reactions listed in section (*a*) of table 1. The rate of reaction (5) is measured *in situ* by monitoring the Cl_2 decay in the photolysis of Cl_2, H_2 and O_2 mixtures. Reaction (3) has previously been studied under the same experimental conditions using the same apparatus. The rate of reaction (4) was measured in this study and its value was in agreement with more exhaustive studies of the photolysis of Cl_2 and Cl_2O with O_2 present.[18] The simulation is relatively insensitive to the value used for k_{11}, as the effective first-order loss for H atoms by this reaction is typically $2 \times 10^6\ s^{-1}$. As described earlier, the ratio k_2/k_{10} was determined under conditions for which the simulation was insensitive to the value used for k_1. The principal uncertainty in the value obtained for k_2 is the estimated error for the value of k_{10}. The 30% error on the mean value of k_{10} covers the range of uncertainties in the four investigations[19-22] on which it is based. The error on the value for k_2 is a combination of this error and the random error in the experimental data [see fig. 4(*a*)].

The determination of k_1 depends principally on the parameters k_2/k_{10}, k_3, k_4 and k_5, and upon the measurement of the concentrations of the reactants. The uncertainties of these quantities are reflected in the simulation of the experiments and subsequent fitting of k_1 to the experimental data. The error quoted for k_1 is estimated from the sum of the squares of residuals plotted in fig. 8.

The value obtained for k_2 in this study implies that reaction (2) is a rapid process occurring at almost every collision. This result is approximately two orders of magnitude greater than that reported previously by Basco and Dogra,[23] in their flash photolysis investigation of Cl_2, Cl_2O mixtures. Their analysis and resultant value for k_1 necessitates an accurate knowledge of the initial [Cl] producted by their flash. This concentration is assumed to be the same as the initial [ClO], which is obtained by extrapolation of the [ClO] to zero time in the experiment. Measurement of initial concentrations is not a trivial problem in flash photolysis, and may in part account for the discrepancy between the molecular modulation and flash-photolysis results. A recent direct measurement of k_2, using the discharge flow technique with detection of species by resonance fluorescence and mass spectrometry,[24] gave

$$k_2 = (9.8 \pm 0.6) \times 10^{-11}\ \text{cm}^3\ \text{molecule}^{-1}\ \text{s}^{-1}\ \text{at 298 K}.$$

This value is in good agreement with the high-pressure result reported here, and therefore implies that there is no apparent pressure dependence of k_2 between a few Torr of He and 1 atm of a mixture of H_2, O_2 and N_2, which is expected for such a rapid reaction.

All three recent investigations of k_1 used the discharge-flow technique operating in the range 1-6 Torr total pressure, and the rate coefficients were determined under pseudo-first-order conditions. Reimann and Kaufman[9] converted HO_2 to OH and ClO to Cl, close to the observation region by reaction with NO,

$$HO_2 + NO \rightarrow NO_2 + OH \tag{20}$$

$$ClO + NO \rightarrow NO_2 + Cl. \tag{21}$$

The OH and Cl were subsequently monitored by resonance fluorescence. These authors obtained a value of $k_1 = (3.8 \pm 0.5) \times 10^{-12}$ cm^3 molecule^{-1} s^{-1} at 298 K. Stimple *et al.*[10] observed HO_2 and ClO directly by l.m.r., and measured k_1 over the range $235 < T < 393$ K, and obtained the following expression for k_2

$$k_2 = 3.3 \times 10^{-11} \exp(-850/T) + 4.5 \times 10^{-12} (T/300)^{-3.7}. \tag{C}$$

This result indicates that k_2 has a complicated temperature dependence. As a possible explanation of the second term on the right-hand side of eqn (C), the authors suggest that formation of complex intermediates may occur:

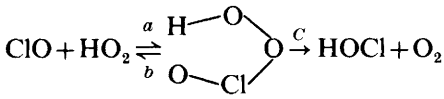

(I)

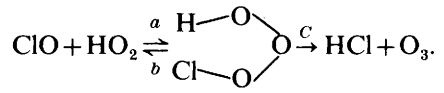

(II)

Using bond additivity rules the bond dissociation energies of the adducts were estimated

$$D(HO_2\text{—}ClO) \approx 15 \text{ kcal mol}^{-1}$$

$$D(HO_2\text{—}OCl) \approx 2 \text{ kcal mol}^{-1}.$$

This implies that mechanism (I) is much more favourable than mechanism (II). Leck *et al.*[11] in their study of reaction (1) detected species by mass spectrometry. [ClO] was measured by observing the change in the Cl_2 signal produced by switching on a microwave discharge, which generates Cl atoms the precursor of ClO. [HO_2] was monitored by converting it to HOCl by the addition of excess ClO

$$k_1 = (4.5 \pm 0.9) \times 10^{-12} \text{ cm}^3 \text{ molecule}^{-1} \text{ s}^{-1} \text{ at 298 K}.$$

They also attempted to observe HCl and O_3, and thereby derived an upper limit for k_{1b},

$$k_{1b} < 1 \times 10^{-13} \text{ cm}^3 \text{ molecule}^{-1} \text{ s}^{-1} \text{ at 298 K}$$

which was based on the apparent absence of these products.

Recently Leu has investigated the product distribution of reaction (1)[25] using the discharge-flow technique with mass spectrometric detection of products. HOCl was observed, but no signals for O_3 were obtained. The mass spectrometer used was not

sensitive enough to detect the products O_2 or HCl. The following upper limits for k_{1b} were obtained

$$k_{1b} < 0.015\, k_1 \text{ at } 298 \text{ K}$$

$$k_{1b} < 0.03\, k_1 \text{ at } 248 \text{ K}.$$

At 298 K the limit is similar to that derived by Leck *et al.*

Fu Su *et al.*[26] investigated the infrared spectrum of HOCl, generating HOCl *via* reaction (1) in the photolysis of Cl_2, O_3 and H_2 mixtures. The infrared band intensities obtained assuming a value for k_{1a} of *ca.* 7×10^{-12} cm^3 molecule^{-1} s^{-1} at 298 K were in agreement with those obtained preparing HOCl by the reaction of H_2O with Cl_2O.[27]

Comparison of the high pressure value of k_2 reported here and the values for k_2 obtained at low pressure, suggest that k_2 is independent of pressure between pressures of a few Torr of He and 1 atm of H_2, O_2 and N_2. However, owing to the sizeable uncertainty on k_2 in this study and the spread of values obtained for k_2 by the discharge-flow technique, some small pressure dependence of reaction (1) cannot be entirely ruled out.

The upper limit presented here for k_{1b} is approximately a factor of 7 lower than the previously reported values. The O_3 produced appeared to be generated by the formation and subsequent photolysis of OClO. Therefore the true value for k_{1b} is probably much lower than this upper limit. This result indicates that mechanism (II) for reaction between HO_2 and ClO must be a very minor channel if it occurs at all. Combining this inference with the observation of HOCl produced *via* reaction (1) at high pressure,[26] and the temperature dependence of k_1,[10] strongly suggests that HOCl is formed by two pathways. The first proceeds *via* an H-atom transfer mechanism, and the second involves the formation of a shortlived HO_2—ClO adduct.

The technique described here for measurement of k_1 is sensitive to radical termination steps such as

$$HO_2 + ClO \rightarrow \text{products}.$$

Any reaction between HO_2 and ClO producing shortlived products ($t_{\frac{1}{2}} < 0.02$ s) which subsequently dissociate to reform HO_2 and ClO would not be measured by the experiments using the molecular-modulation techniques presented here. One such pathway might be the possible endothermic route (1*c*) followed by dissociation:

$$HO_2 + ClO \rightarrow HClO + O_2 \qquad (1c)$$

$$HClO \rightarrow H + ClO \qquad (22)$$

$$H + O_2 + M \rightarrow HO_2 + M. \qquad (11)$$

In the stratosphere if HOCl is the product of reaction (1), then this reaction is an apparent sink for ClO_x species. However recent investigations of the u.v. spectrum of HOCl[28, 29] indicate appreciable absorption in the 300-400 nm region. Consequently the stratospheric daytime lifetime of HOCl is < 30 min.[10] Nevertheless, reaction (1) remains an important stratospheric reaction as O_3 can be destroyed catalytically *via* the reactions

$$ClO + HO_2 \rightarrow HOCl + O_2$$

$$HOCl + h\nu \rightarrow OH + Cl$$

$$OH + O_3 \rightarrow HO_2 + O_2$$

$$Cl + O_3 \rightarrow ClO + O_2$$

$$\text{- - - - - - - - - - - - - - - - - -}$$

$$O_3 + O_3 \rightarrow O_2 + O_2 + O_2.$$

This scheme is particularly important in the middle and lower stratosphere.

This work was funded by the Department of the Environment. The authors are indebted to Dr R. G. Derwent for assistance in computer simulation of the chemical system and for many useful discussions.

[1] M. J. Molina and F. S. Rowland, *Nature (London)*, 1974, **249**, 810.
[2] *Chlorofluorocarbons and their Effect on Stratospheric Ozone*, Pollution Report No. 15 (H.M.S.O., London, 1979).
[3] *Stratospheric Ozone Depletion by Halocarbons: Chemistry and Transport* (National Academy of Science, Washington, D.C., 1979).
[4] E. J. Hamilton, *J. Chem. Phys.*, 1975, **63**, 3682.
[5] R. A. Cox and J. P. Burrows, *J. Phys. Chem.*, 1979, **83**, 2560.
[6] J. P. Burrows, D. I. Cliff, E. W. Harris, B. A. Thrush and J. P. T. Wilkinson, *Proc. R. Soc. London, Ser. A*, 1979, **368**, 463.
[7] R. A. Cox and R. G. Derwent, *J. Chem. Soc., Faraday Trans. 1*, 1979, **75**, 1635.
[8] N. Basco and J. E. Hunt, *Int. J. Chem. Kinet.*, 1979, **11**, 649.
[9] B. Reimann and F. Kaufman, *J. Chem. Phys.*, 1978, **69**, 2925.
[10] R. H. Stimpfle, R. A. Perry and C. J. Howard, *J. Chem. Phys.*, 1978, **71**, 5183.
[11] T. J. Leck, J. L. Cook and J. W. Birks, *J. Chem. Phys.*, 1980, **72**, 2364.
[12] M. C. Addison, J. P. Burrows, R. A. Cox and R. Patrick, *Chem. Phys. Lett.*, 1980, **73**, 283.
[13] R. A. Cox, R. G. Derwent, A. E. J. Eggleton and H. J. Reid, *J. Chem. Soc., Faraday Trans. 1*, 1979, **75**, 1648.
[14] R. T. Watson, *J. Phys. Chem. Ref. Data*, 1977, **6**, 871.
[15] R. A. Cox and R. Lewis, *J. Chem. Soc., Faraday Trans. 1*, 1979, **75**, 2649.
[16] R. A. Cox and R. G. Derwent, *J. Chem. Soc., Faraday Trans. 1*, 1977, **73**, 272.
[17] E. M. Chance, A. R. Curtis, I. P. Jones and C. R. Kirby, *FACSIMILE: a Computer Program for Flow and Chemistry Simulation and General Initial-value Problems* (A.E.R.E. Report A.E.R.E. R 8775, H.M.S.O., London, 1977).
[18] M. C. Addison, J. P. Burrows and R. A. Cox, to be published.
[19] D. D. Davis, W. Brown and A. Bass, *Int. J. Chem. Kinet.*, 1970, **2**, 101.
[20] P. F. Ambridge, J. N. Bradley and D. A. Whytock, *J. Chem. Soc., Faraday Trans. 1*, 1976, **72**, 2143.
[21] J. H. Lee, J. V. Michael, W. A. Payne, L. J. Stief and D. A. Whytock, *J. Chem. Soc., Faraday Trans. 1*, 1977, **73**, 1530.
[22] R. T. Watson, E. S. Machado, R. L. Schiff, S. Fischer and D. D. Davis, in preparation.
[23] N. Basco and S. K. Dogra, *Proc. R. Soc. London, Ser. A*, 1971, **323**, 401.
[24] M. T. Leu and R. T. Watson, *J. Phys. Chem.*, 1980, **84**, 1674.
[25] M. T. Leu, *Geophys. Res. Lett.*, 1980, **7**, 173.
[26] Fu Su, J. G. Calvert, C. R. Lindley, W. M. Uselman and J. H. Shaw, *J. Phys. Chem.*, 1980, **83**, 913.
[27] P. D. Maker, H. Niki, C. M. Savage and L. P. Breitenbach, Paper 80 presented at the *Symposium on Fourier Transform Spectroscopic Studies of Atmospheric and Interstellar Species*, 176th Meeting of the American Chemical Society, Miami, U.S.A., 1978.
[28] L. T. Molina and M. J. Molina, *J. Phys. Chem.*, 1978, **82**, 2410.
[29] S. Jaffe and W. B. DeMore, unpublished work quoted in S. Prasad, L. Jaffe, C. Whitten and R. P. Turco, *Plant. Space Sci.*, 1978, **26**, 1017.
[30] A. W. Miziolek and M. J. Molina, *J. Phys. Chem.*, 1978, **82**, 1769.
[31] D. L. Baulch, R. A. Cox, R. F. Hampson Jr, J. A. Kerr, J. Troe and R. T. Watson, *J. Phys. Chem. Ref. Data*, 1980, **9**, 295.

(PAPER 0/1472)